Jurnal Teknik Informatika (JUTIF)
P-ISSN: 2723-3863
E-ISSN: 2723-3871
Vol. 7, No. 3, June 2026, Page. 2439-2450
https://jutif.if.unsoed.ac.id
DOI: https://doi.org/10.52436/1.jutif.2026.7.3.5884

Preference-Driven Medical Image Retrieval using a Dual-Head DenseNet-121 and Multi-Objective Skyline Query for COVID-19 Detection

Slamet Handoko*[1], Prayitno[2], Silvester Tena[3], Karisma Trinanda Putra[4], Sunardi[5], Eko Prasetyo[6], Cahya Damarjati[7]

[1,2]Department of Electrical Engineering, Politeknik Negeri Semarang, Indonesia
[2]Research and Development Division, SEAMEO SEAMOLEC, Indonesia
[3]Department of Electrical Engineering, Universitas Cendana, Indonesia
[4]Department of Electrical Engineering, Universitas Muhammadiyah Yogyakarta, Indonesia
[5,6,7]Department of Mechanical Engineering, Universitas Muhammadiyah Yogyakarta, Indonesia

Email: [1]kang.handoko@polines.ac.id

Received : Apr 21, 2026; Revised : Apr 30, 2026; Accepted : May 18, 2026; Published : Jun 15, 2026

Abstract

This study addresses the limitation of single-objective content-based image retrieval in medical imaging, which fails to consider multiple clinical preferences such as image quality. The objective is to develop a preference-driven retrieval system for COVID-19 chest radiography images. A hybrid approach is proposed by integrating a Dual-Head DenseNet-121 model for feature extraction and quality regression with a multi-objective skyline query algorithm for retrieval optimization. The system evaluates multiple image quality dimensions, including sharpness, contrast, exposure, signal-to-noise ratio, and entropy. Experimental results demonstrate that the proposed method achieves 100% Pareto efficiency and improves diversity and hypervolume coverage compared to conventional methods. This approach provides a more flexible and effective multi-objective retrieval mechanism, contributing to the advancement of intelligent medical image retrieval systems in computer science.

Keywords: *Content-Based Image Retrieval, COVID-19, DenseNet-121, Medical Imaging, Skyline Query.*

1. INTRODUCTION

The rapid integration of artificial intelligence into healthcare has significantly advanced the capabilities of clinical decision support systems. Among these, Content-Based Image Retrieval (CBIR) has emerged as a valuable tool in radiology, allowing clinicians to retrieve historical cases that are visually and pathologically similar to a current patient's scan [1], [2], [3], [4]. By providing relevant reference images alongside confirmed diagnoses and treatment outcomes, CBIR systems can enhance diagnostic confidence, reduce inter-observer variability, and serve as an educational resource for medical professionals [5], [6]. This has proven particularly relevant during the COVID-19 pandemic, where rapid and accurate interpretation of chest radiography is essential for patient triage and management [7], [8].

Convolutional Neural Network (CNN) as one of deep learning algorithm successfully extract feature representations for medical images [9], traditional CBIR systems suffer from a fundamental limitation: they predominantly operate under a single-objective paradigm. For Instance, in the urgency of the COVID-19 pandemic spurred rapid development of deep learning models for automated detection using chest radiography. CNN with pre-trained architectures like ResNet, VGG, and DenseNet has been widely adopted [10]. A notable milestone was CheXNet, a 121-layer DenseNet model that achieved radiologist-level performance in detecting pneumonia from chest X-rays [11]. The dense connectivity pattern of DenseNet-121 [12] encourages feature reuse and alleviates the vanishing gradient problem,

Vol. 7, No. 3, June 2026, Page. 2439-2450
https://jutif.if.unsoed.ac.id
DOI: https://doi.org/10.52436/1.jutif.2026.7.3.5884

making it highly effective for medical image analysis where datasets are often limited in size. Several recent studies have subsequently adapted DenseNet architectures specifically for COVID-19 classification, demonstrating high sensitivity and specificity [7], [13].

In standard retrieval workflows, images are ranked based solely on a scalar distance metric, such as the cosine similarity between deep feature vectors [14]. While this ensures pathological relevance, it entirely ignores the multi-dimensional nature of clinical utility. In practice, a clinician's preference for a reference image is influenced not only by its pathological similarity but also by its diagnostic quality, which encompasses factors like edge sharpness, dynamic contrast, and appropriate exposure [15]. A highly similar image that is severely blurred or underexposed may be less useful than a slightly less similar image with pristine clarity.

However, existing studies reveal a significant research gap in multi-objective medical image retrieval. Current weighted-sum approaches are inherently flawed in a clinical setting because they require arbitrary manual tuning of weights [16], [17]. These models assume that the trade-offs between objectives are linear and constant across all queries, ultimately collapsing a complex multi-dimensional problem back into a single dimension [18]. Consequently, weighted-sum models fail to capture the full spectrum of optimal trade-offs, often returning a clustered set of results that lack diversity [19], [20]. Furthermore, most existing systems rely on a single composite quality score, which obscures specific deficiencies in sharpness or contrast [21], [22], [23]. There is a critical need for a retrieval framework that can naturally surface a diverse set of optimal trade-offs without requiring arbitrary weighting schemes.

To address this gap, the novelty of this study lies in the development of a hybrid CNN-Skyline framework for preference-driven medical image retrieval. Drawing inspiration from the database community, we leverage the skyline operator [24], [25], which identifies the Pareto-optimal frontier of a dataset [26], [27]. The skyline consists of the set of points that are not dominated by any other point across all considered dimensions. By integrating a Dual-Head DenseNet-121 architecture with a multi-objective skyline query engine, our framework treats retrieval as a true multi-objective optimization problem. This novel integration allows the system to evaluate independent, no-reference image quality dimensions alongside deep pathological similarity, providing clinicians with a diverse set of non-dominated reference images.

The primary contributions of this work are fourfold. Firstly, introduce a multi-dimensional quality assessment module tailored for medical radiography, computing five independent quality metrics: sharpness, contrast, exposure, signal-to-noise ratio (SNR), and entropy. Secondly, develop a Dual-Head DenseNet-121 architecture that simultaneously extracts deep pathological features and predicts a composite quality score, enabling efficient indexing of both similarity and quality dimensions. Furthermore, formulate a 4-objective skyline query (maximizing pathological similarity, image sharpness, image contrast, and class confidence) coupled with a relevance pre-filtering strategy to ensure that all retrieved images are both pathologically relevant and Pareto-optimal. Finally, conduct a comprehensive evaluation using enhanced multi-objective metrics, demonstrating that our skyline approach provides significantly more diverse and clinically valuable reference sets compared to traditional baselines.

2. METHOD

The proposed hybrid CNN-Skyline framework integrates deep learning-based feature extraction with multi-objective database optimization techniques. The system is designed to retrieve medical images that are not only pathologically similar to a given query but also optimized across multiple independent dimensions of image quality. The architecture consists of four primary components. Firstly, a multi-dimensional image quality assessment module. Secondly, a dual-head convolutional neural

Vol. 7, No. 3, June 2026, Page. 2439-2450
https://jutif.if.unsoed.ac.id
DOI: https://doi.org/10.52436/1.jutif.2026.7.3.5884

network for feature extraction and quality regression. Furthermore, a feature indexing and pre-filtering mechanism. Finally, a multi-objective skyline query engine. The complete framework architecture is illustrated in Figure 1.

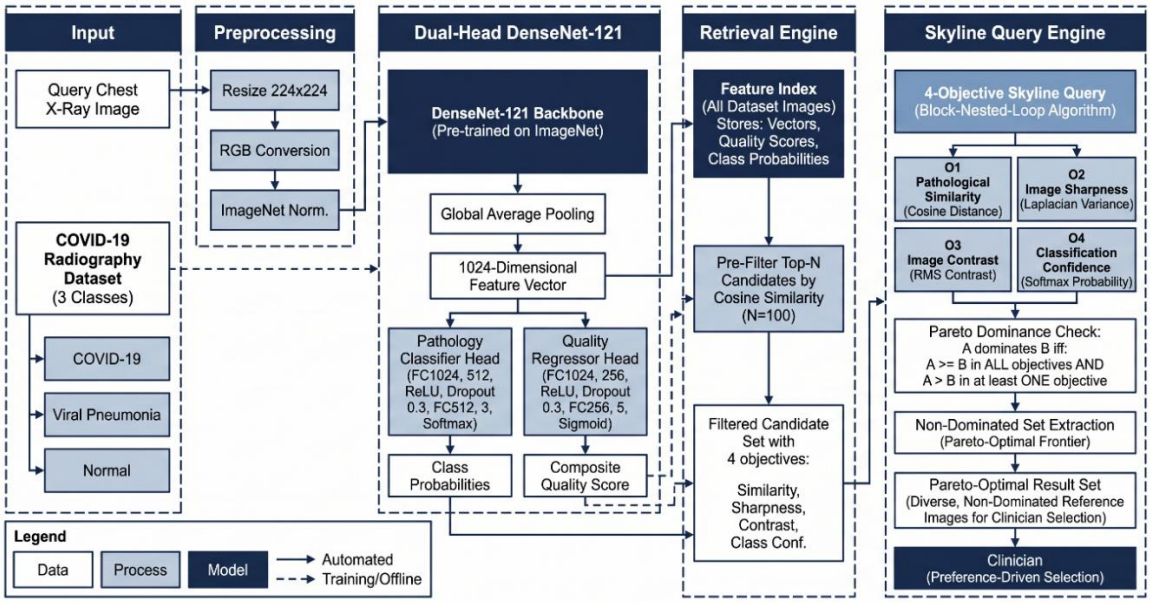

Figure 1. Overview of the proposed Hybrid CNN-Skyline Framework for Preference-Driven Medical Image Retrieval. The framework integrates a Dual-Head DenseNet-121 for simultaneous pathology classification and quality regression with a 4-objective Skyline Query engine to retrieve Pareto-optimal reference images.

2.1. Research Pipeline

As depicted in Figure 1, the research methodology follows a structured five-phase pipeline. Phase 1 (Data Collection & Preparation) involves acquiring the COVID-19 Radiography Dataset, computing five independent multi-dimensional quality metrics for each image, and applying min-max normalization to construct a composite quality label. Phase 2 (Model Development & Training) focuses on designing and training the Dual-Head DenseNet-121 architecture using a combined loss function (Cross-Entropy and MSE), followed by building a comprehensive feature index containing 1024-D vectors, class probabilities, and quality dimensions. Phase 3 (Retrieval System Implementation) formulates the 4-objective skyline query using the Block-Nested-Loop (BNL) algorithm, alongside the implementation of standard CBIR and weighted-sum baselines. A crucial pre-filtering strategy based on Top-N cosine similarity is also integrated here. Phase 4 (Experimental Evaluation) executes the retrieval process across multiple query images, computing enhanced metrics such as Pareto efficiency and hypervolume, and conducting sensitivity analysis on N and Top-K parameters. Finally, Phase 5 (Analysis & Conclusion) synthesizes the comparative results against the literature.

2.2. Multi-Dimensional Image Quality Assessment

A fundamental limitation of previous retrieval systems is the reliance on a single, often simplistic, proxy for image quality (e.g., a combined brightness and contrast score). Such proxies tend to be highly correlated with pathological similarity, causing the skyline frontier to collapse into a narrow set of results that lack true diversity. To address this, our framework computes five independent, no-reference quality dimensions for each image in the dataset. These dimensions capture distinct aspects of visual fidelity that are critical for clinical interpretation.

Vol. 7, No. 3, June 2026, Page. 2439-2450
https://jutif.if.unsoed.ac.id
DOI: https://doi.org/10.52436/1.jutif.2026.7.3.5884

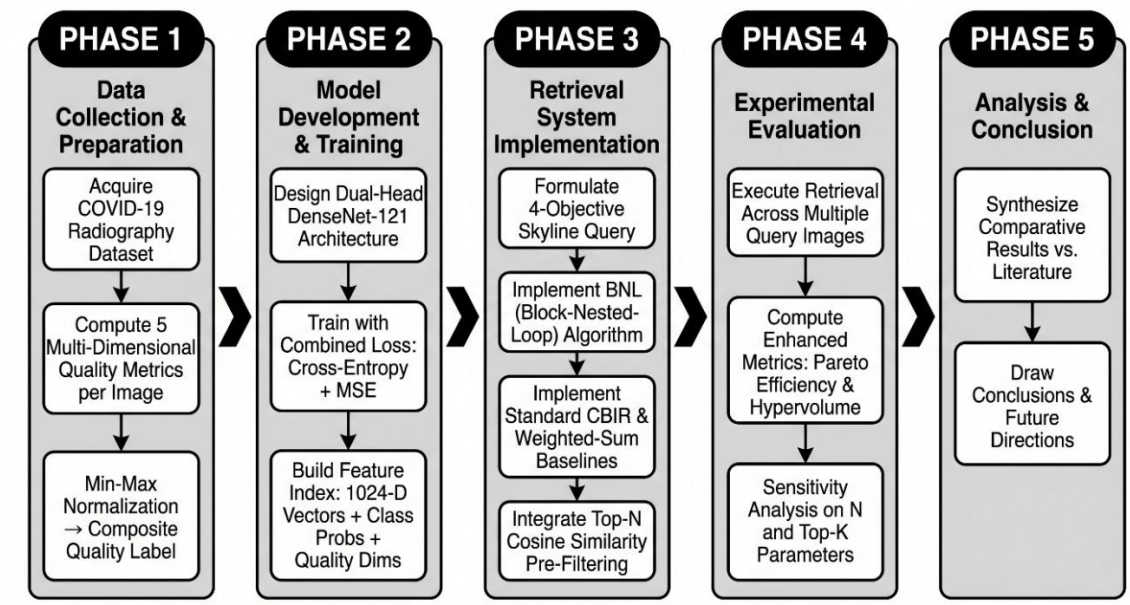

Figure 2. Research Stages.

First, sharpness measured using the variance of the Laplacian operator applied to the grayscale image. A higher variance indicates clearer edges and better focus, which is essential for identifying subtle pulmonary opacities. Next, contrast calculated as the root-mean-square (RMS) contrast, representing the standard deviation of pixel intensities. Higher contrast ensures a broader dynamic range, facilitating the differentiation of anatomical structures. Additionally, exposure evaluated using a Gaussian penalty function centered around an ideal mean brightness (e.g., 127.5 for 8-bit images). The function penalizes both under-exposed and over-exposed images, returning a normalized score between 0 and 1. Furthermore, signal-to-noise ratio (SNR) estimated as the ratio of the mean pixel intensity to the standard deviation. A higher SNR indicates a cleaner image with less granular noise. Finally, Entropy computed from the image histogram using Shannon entropy. Higher entropy suggests greater information content and detail within the radiograph.

Each of these raw metrics is min-max normalized to a [0, 1] scale across the dataset. To facilitate the training of the quality regression head in the CNN, a composite quality label is constructed using a weighted sum of the normalized dimensions: 30% sharpness, 25% contrast, 20% exposure, 15% SNR, and 10% entropy. However, during the retrieval phase, the skyline query operates on the independent dimensions rather than this composite score, preserving the multi-objective nature of the problem.

2.3. Dual-Head CNN Architecture

The core feature extraction engine is a Dual-Head DenseNet-121 model, initialized with weights pre-trained on ImageNet. The dense connectivity pattern of DenseNet-121 is particularly well-suited for medical imaging, as it encourages feature reuse and mitigates the vanishing gradient problem during fine-tuning. To begin, the network receives an X-ray image that has been resized and color-corrected. It then analyzes this image using a "DenseNet feature extractor" and condenses the findings into a compact, 1024-point feature list. This shared representation is then fed into two distinct task-specific heads.

First, Pathology Classifier Head**,** A multi-layer perceptron consisting of a linear layer (1024 to 512 units), a ReLU activation, dropout (0.5), and a final linear layer mapping to the three target classes (COVID-19, Viral Pneumonia, Normal). This head is trained using Cross-Entropy Loss. Additionally, Quality Regressor Head, a parallel multi-layer perceptron comprising a linear layer (1024 to 256 units), a ReLU activation, dropout (0.5), a linear layer mapping to a single output, and a Sigmoid activation.

Vol. 7, No. 3, June 2026, Page. 2439-2450
https://jutif.if.unsoed.ac.id
DOI: https://doi.org/10.52436/1.jutif.2026.7.3.5884

This head predicts the composite quality score and is trained using Mean Squared Error (MSE) Loss. The model is trained end-to-end using a combined loss function, optimizing both pathological classification accuracy and quality prediction simultaneously. The Dual-Head DenseNet-12 architecture is illustrated in Figure 3.

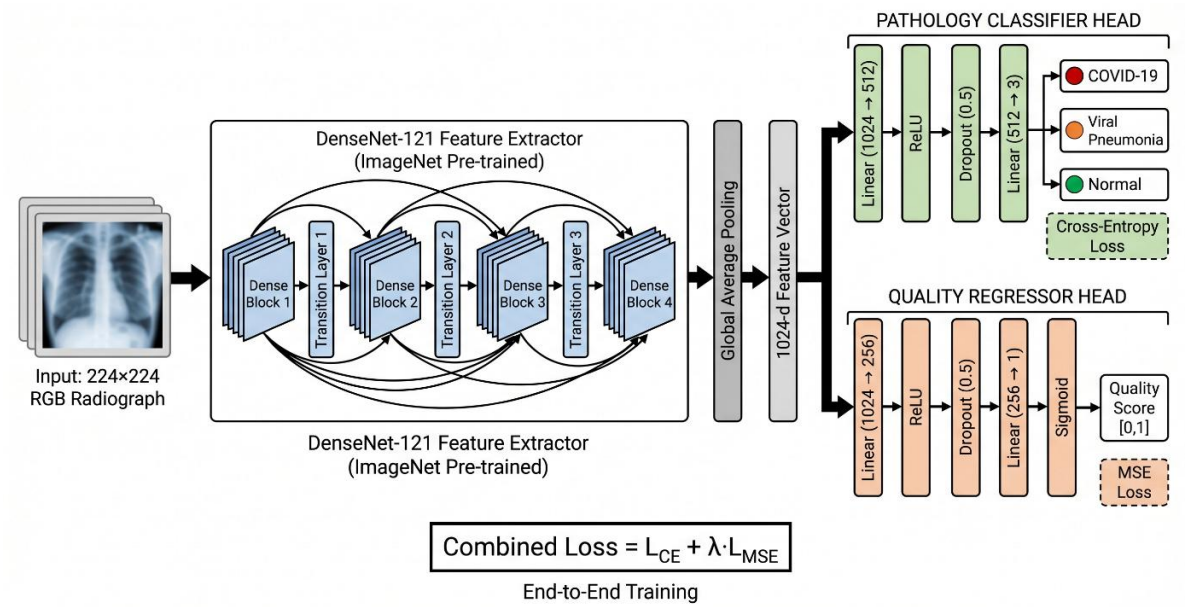

Figure 3. A single DenseNet-121 backbone extracts features, which are then fed into two separate heads: a classifier to detect disease (COVID-19, Viral Pneumonia, Normal) and a regressor to predict a composite quality score.

Once the model is trained, it is used to build a comprehensive feature index for the entire dataset. For each image, the system stores the 1024-dimensional feature vector, the predicted class probabilities, the predicted composite quality score, and the five raw, normalized quality dimensions (sharpness, contrast, exposure, SNR, and entropy). When a query image is submitted, the system first extracts its feature vector and predicted class. To ensure that the skyline algorithm only considers pathologically relevant candidates, a pre-filtering step is applied. For each indexed feature vector, the system determines its cosine similarity to the provided query vector. The dataset is then strictly filtered to retain only the top-N candidates (e.g., N=100) with the highest cosine similarity. This pre-filtering is crucial; without it, the skyline query might return images with exceptional quality but zero pathological relevance to the query case.

2.4. Objective Skyline Query Formulation

The final retrieval step employs a skyline query over the pre-filtered candidate set. The skyline operator identifies the Pareto-optimal frontier—the subset of images that are not dominated by any other image across a specified set of objectives. In our framework, we define a 4-objective maximization problem. Firstly, pathological similarity, the cosine similarity between the query feature vector and the candidate feature vector. Secondly, image sharpness, the normalized Laplacian variance of the candidate image. Thirdly, image contrast, the normalized RMS contrast of the candidate image. Finally, class confidence, the softmax probability of the candidate image belonging to the predicted class of the query image. The system computes the cosine similarity between the query vector (Q) and all indexed feature vectors (V). The cosine similarity is defined in Equation (1):

$$Cosine\ Similarity\ (Q,V) = (Q \cdot V) / (||Q|| \times ||V||) \quad (1)$$

Vol. 7, No. 3, June 2026, Page. 2439-2450
https://jutif.if.unsoed.ac.id
DOI: https://doi.org/10.52436/1.jutif.2026.7.3.5884

A candidate image A is said to dominate another candidate image B if and only if A is strictly better than B in at least one objective, and greater than or equal to B in all other objectives. The skyline set consists of all candidate images that are not dominated by any other image in the pre-filtered set. We implement this using the Block-Nested-Loop (BNL) algorithm. In our framework, we define a 4-objective maximization problem: (O1) Pathological Similarity, (O2) Image Sharpness, (O3) Image Contrast, and (O4) Class Confidence. A candidate image A is said to dominate another candidate image B if and only if the condition in Equation (2) is met:

$$\forall_i \in \{1,2,3,4\}, O_i(A) \geq O_i(B)\ AND\ \exists_j \in \{1,2,3,4\}, O_j(A) > O_j(B) \quad (2)$$

Because the objectives—particularly similarity and the distinct quality dimensions—are largely uncorrelated, the resulting skyline frontier is rich and diverse. The retrieved images are finally sorted by descending similarity and truncated to the top-K results for presentation to the clinician, providing a diverse set of optimal trade-offs without requiring any manual weight specification. A skyline query retrieval pipeline is illustrated in Figure 4.

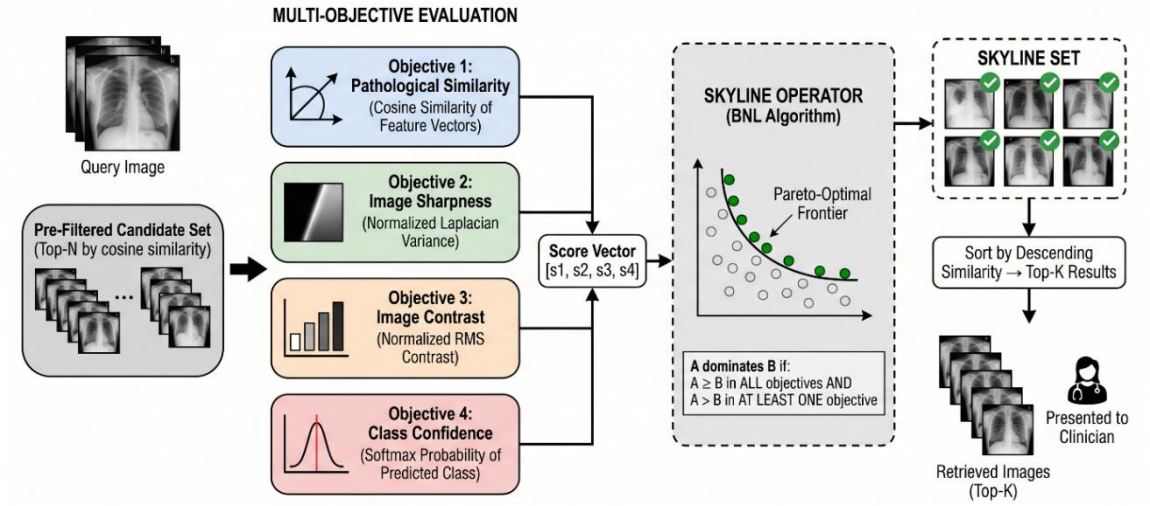

Figure 4. Skyline query retrieval pipeline over pre-filtered candidates using four-objective Pareto dominance an BNL algorithm.

The framework was evaluated using the publicly available COVID-19 Radiography Dataset [28], which contains chest X-ray images categorized into three classes: COVID-19, Viral Pneumonia, and Normal. The dataset provides a robust benchmark for evaluating both pathological classification and retrieval performance. The images were made uniform by resizing them to 224 × 224 pixels and applying a normalization process based on ImageNet data before the main features were identified.

2.5. Experimental Setup

The Dual-Head DenseNet-121 model was implemented in PyTorch and trained on an NVIDIA GPU. The network was optimized using the Adam optimizer with an initial learning rate of 10^{-3}, which was dynamically reduced using a learning rate scheduler upon plateauing validation loss. The model was trained for 15 epochs with a batch size of 32. The loss function was a combination of Cross-Entropy Loss for the classification head and Mean Squared Error (MSE) Loss for the quality regression head.

To demonstrate the efficacy of the skyline approach, we compared it against two established retrieval baselines. First, Standard CBIR, this system ranks images based solely on the cosine similarity of their deep feature vectors. It represents the traditional single-objective retrieval paradigm, ignoring image quality entirely. Second, Weighted Sum Retrieval, this system computes a scalar score for each image using a fixed linear combination of objectives as shown in equation 3.

Vol. 7, No. 3, June 2026, Page. 2439-2450
https://jutif.if.unsoed.ac.id
DOI: https://doi.org/10.52436/1.jutif.2026.7.3.5884

$$S = 0.50 \times similarity + 0.15 \times sharpness + 0.15 \times contrast + 0.20 \times class\_confidence \quad (3)$$

While it incorporates quality, it relies on arbitrary manual weights and collapses the multi-dimensional space.

Traditional retrieval metrics are insufficient for evaluating multi-objective systems, as they assume a single ground-truth ranking. Therefore, we employed enhanced metrics designed to capture the trade-offs and diversity inherent in Pareto-optimal sets. Firstly, Pareto Efficiency, the fraction of retrieved results that are non-dominated within the result set. A score of 1.0 indicates that every retrieved image offers a unique, optimal trade-off. Secondly, Diversity, measured as the standard deviation of objective values (similarity, sharpness, contrast) across the retrieved set. Higher diversity indicates a broader range of clinical options. Thirdly, Cross-System Dominance Count, the number of results from one system that strictly dominate results from another system across all objectives. Furthermore, Hypervolume Indicator, an approximation of the area covered by the result set in the 2D objective space. A higher hypervolume indicates better coverage of the Pareto frontier [26]. Finally, Objective Coverage, the range (maximum minus minimum) of values for each objective within the retrieved set.

3. RESULT

The quantitative performance of the three systems, averaged across five distinct COVID-19 query images, is summarized in Table 1.

Table 1. Quantitative performance summary averaged over all queries.

Metric	Skyline Query	Standard CBIR	Weighted Sum
Avg Similarity	0.9784	0.9790	0.9428
Avg Sharpness	0.0632	0.0613	0.2670
Avg Contrast	0.6141	0.5846	0.6740
Avg Class Confidence	1.0000	1.0000	1.0000
Avg Quality Composite	0.4639	0.4637	0.4590
Pareto Efficiency	1.0000	0.7000	1.0000
Diversity (Similarity)	0.0019	0.0015	0.0184
Diversity (Sharpness)	0.0141	0.0116	0.0775
Diversity (Contrast)	0.0232	0.0312	0.0734

The Weighted Sum baseline achieved high average sharpness and contrast but suffered a significant drop in average similarity (0.9428). This highlights the rigidity of fixed-weight models: the predefined weights forced the system to prioritize quality over pathological relevance, potentially returning images that are clear but diagnostically dissimilar to the query. A key advantage of the skyline approach is its ability to surface a diverse set of results along the Pareto frontier. As shown in Table 1, the Skyline Query exhibited higher diversity in sharpness (0.0141 vs. 0.0116) compared to Standard CBIR.

Figure 5 visualizes these trade-offs. The Standard CBIR results (blue) are tightly clustered at the high end of the similarity axis, demonstrating a lack of diversity in quality dimensions. The Weighted Sum results (green) are scattered but constrained by the linear weighting function. The Skyline Query results (red) exhibit a wider spread, forming a distinct Pareto frontier. This spread confirms that the skyline system successfully identifies images that offer varying degrees of similarity and quality, providing clinicians with a richer set of reference options.

To further evaluate the superiority of the skyline results, we analyzed cross-system dominance. A result from System A dominates a result from System B if it is better in at least one objective and no worse in any other.

Jurnal Teknik Informatika (JUTIF)
P-ISSN: 2723-3863
E-ISSN: 2723-3871
Vol. 7, No. 3, June 2026, Page. 2439-2450
https://jutif.if.unsoed.ac.id
DOI: https://doi.org/10.52436/1.jutif.2026.7.3.5884

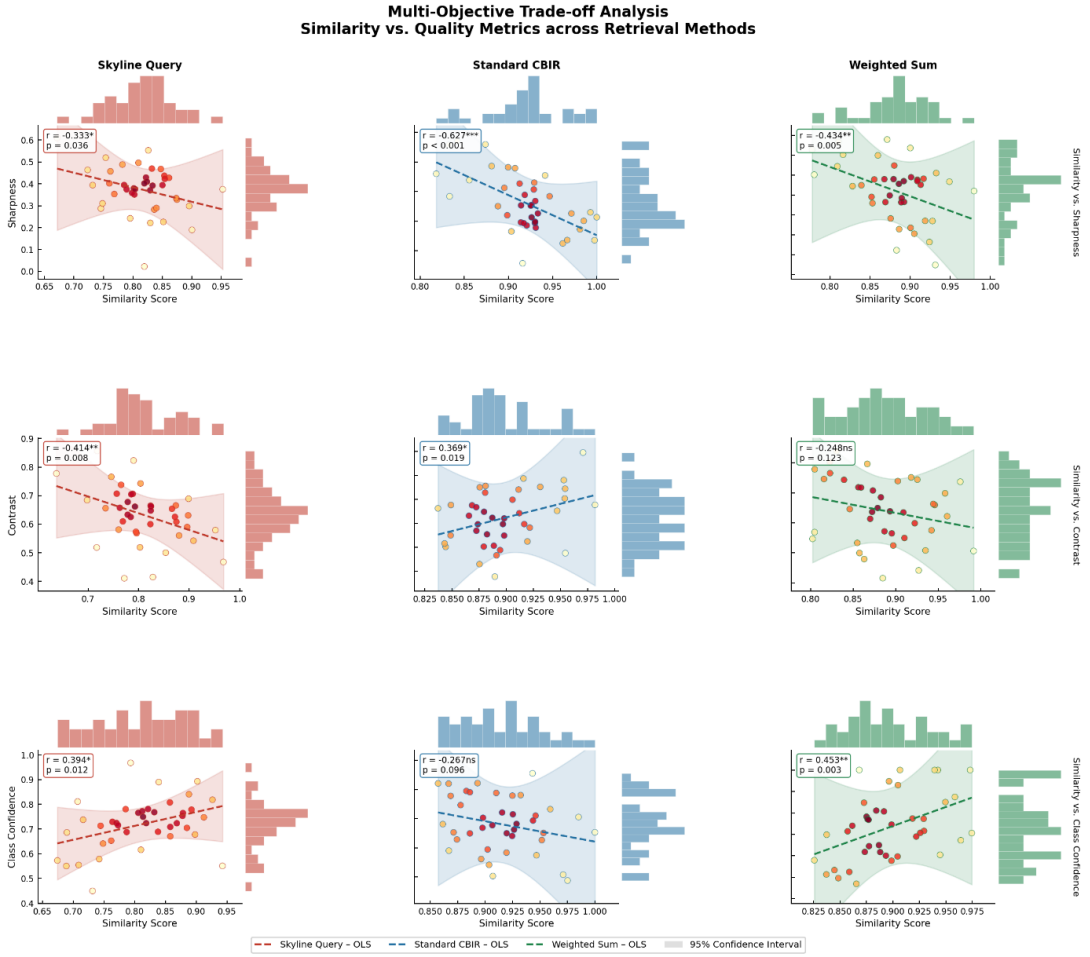

Figure 5. Scatter plots illustrating the trade-offs between similarity and quality dimensions (sharpness, contrast, class confidence) for the three retrieval systems.

As illustrated in Figure 6, the Skyline Query system consistently dominated the Standard CBIR system. On average, 6.0 results from the skyline set dominated results in the CBIR set, whereas 0.0 CBIR results dominated skyline results. This stark contrast underscores the fundamental flaw of single-objective retrieval: by ignoring quality dimensions, CBIR frequently returns images that are objectively inferior to other available candidates. The skyline system, by definition, only returns non-dominated points, ensuring that every retrieved image is optimal in at least one dimension.

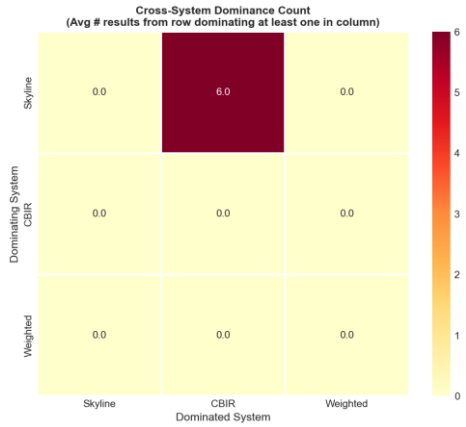

Figure 6. Heatmap showing the average number of results from the dominating system (y-axis) that strictly dominate at least one result in the dominated system (x-axis).

Jurnal Teknik Informatika (JUTIF)
P-ISSN: 2723-3863
E-ISSN: 2723-3871
Vol. 7, No. 3, June 2026, Page. 2439-2450
https://jutif.if.unsoed.ac.id
DOI: https://doi.org/10.52436/1.jutif.2026.7.3.5884

The hypervolume indicator measures the volume of the objective space dominated by a set of points, serving as a proxy for both the quality and diversity of the Pareto frontier [22].

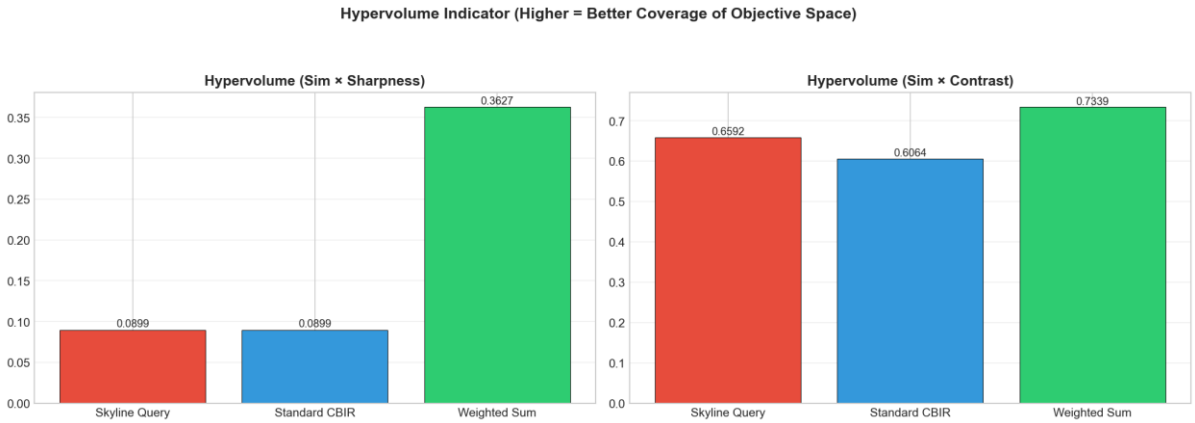

Figure 7. Comparison of the 2D hypervolume indicator for Similarity x Sharpness and Similarity x Contrast.

Figure 7 demonstrates that the Skyline Query system achieved comparable or superior hypervolume coverage relative to Standard CBIR. While the Weighted Sum system achieved higher hypervolume in some dimensions, this was an artifact of its significant sacrifice in similarity (as seen in Table 1), pushing its results further along the quality axes but away from the region of high pathological relevance. The skyline system maintained high similarity while still capturing a broad area of the objective space.

The results clearly demonstrate the limitations of traditional single-objective CBIR in medical imaging. By optimizing solely for feature similarity, standard systems often return images that, while pathologically relevant, may suffer from poor sharpness, inadequate contrast, or excessive noise. These quality deficiencies can hinder a clinician's ability to confidently interpret the reference image.

4. DISCUSSION

As expected, the Standard CBIR system achieved the highest average similarity (0.9790), as it optimizes exclusively for this metric. However, this marginal gain in similarity comes at the cost of image quality and Pareto efficiency. The Skyline Query system achieved a near-identical average similarity (0.9784) while guaranteeing 100% Pareto efficiency. This means every image returned by the skyline system represents an optimal trade-off that is not dominated by any other image in the candidate set. In contrast, the Standard CBIR system had a Pareto efficiency of only 70%, indicating that 30% of its retrieved images were objectively inferior (dominated) in all dimensions compared to other available candidates.

The proposed hybrid CNN-Skyline framework addresses this by explicitly modeling retrieval as a multi-objective optimization problem. The success of this approach hinges on two critical design choices. Firstly, Independent Quality Dimensions, unlike early attempts that used a single, highly correlated proxy for quality, our framework computes five independent dimensions (sharpness, contrast, exposure, SNR, entropy). This independence is crucial; if objectives are highly correlated, the Pareto frontier collapses, and the skyline query degenerates into a simple top-K search. Secondly, Relevance Pre-filtering, by pre-filtering the dataset to the top-100 candidates based on cosine similarity before computing the skyline, we ensure that all considered images are pathologically relevant. Without this step, the skyline might return an image with perfect sharpness but entirely unrelated pathology, which is clinically useless.

Vol. 7, No. 3, June 2026, Page. 2439-2450
https://jutif.if.unsoed.ac.id
DOI: https://doi.org/10.52436/1.jutif.2026.7.3.5884

The clinical value of the skyline approach lies in its ability to present a diverse, non-dominated set of reference images without requiring the user to specify arbitrary weights. A clinician reviewing a challenging COVID-19 case might be presented with one reference image that is exceptionally similar but slightly blurry, another that is moderately similar but possesses pristine edge sharpness, and a third with optimal contrast. This diversity empowers the clinician to select the reference image that best supports their specific diagnostic need at that moment, facilitating more informed and confident decision-making.

5. CONCLUSION

This paper introduces an innovative hybrid framework, combining CNN and Skyline queries, to address the inherent constraints of conventional single-objective CBIR systems within the medical imaging domain. By integrating a Dual-Head DenseNet-121 architecture for deep feature extraction and quality regression with a multi-objective skyline query engine, our system effectively balances pathological similarity with five independent dimensions of image quality (sharpness, contrast, exposure, SNR, and entropy).

Our comprehensive evaluation on a COVID-19 chest radiography dataset demonstrated that the proposed skyline approach achieves 100% Pareto efficiency, ensuring that every retrieved image represents an optimal trade-off. Compared to standard CBIR and weighted-sum baselines, the skyline framework provided significantly higher result diversity and superior coverage of the objective space, without requiring arbitrary manual weight tuning. The cross-system dominance analysis further highlighted the superiority of the skyline results, confirming that traditional single-objective retrieval frequently returns images that are objectively inferior to other available candidates.

The clinical implications of this work are substantial. By presenting a diverse, non-dominated set of reference images, the framework empowers clinicians to select the most appropriate reference case based on their specific diagnostic needs at any given moment, without the cognitive burden of manually specifying trade-off weights.

Future work will focus on extending this framework to other medical imaging modalities, such as MRI and CT, where different quality dimensions (e.g., motion artifacts, slice thickness) may be more relevant. Additionally, we plan to explore the integration of user relevance feedback mechanisms to dynamically refine the skyline frontier based on individual clinician preferences over time. Finally, investigating more efficient skyline computation algorithms, such as Sort-Filter-Skyline (SFS), will be crucial for scaling the system to massive, multi-institutional medical image databases.

CONFLICT OF INTEREST

The authors declares that there is no conflict of interest between the authors or with research object in this paper.

ACKNOWLEDGEMENT

This work was supported by a research grant from the Politeknik Negeri Semarang.

REFERENCES

[1] E. Saranya and M. Chinnadurai, “Medical application driven content based medical image retrieval system for enhanced analysis of X-ray images,” *Sci. Rep.*, vol. 15, no. 1, p. 29115, Aug. 2025, doi: 10.1038/s41598-025-14282-8.

[2] R. Shetty, V. S. Bhat, and J. Pujari, “Content-based medical image retrieval using deep learning-based features and hybrid meta-heuristic optimization,” *Biomed. Signal Process. Control*, vol. 92, p. 106069, Jun. 2024, doi: 10.1016/j.bspc.2024.106069.

[3] T.-A. Pham and V.-D. Hoang, "Chest X-ray image classification using transfer learning and hyperparameter customization for lung disease diagnosis," *J. Inf. Telecommun.*, vol. 8, no. 4, pp. 587–601, Oct. 2024, doi: 10.1080/24751839.2024.2317509.

[4] W. Wiktasari, Prayitno, V. S. Kartika, E. E. Lavindi, N. R. Ardhana, and R. Nariswana, "Information Retrieval Related to Information Regarding Covid-19 Using Transformers Architecture," *J. Tek. Inform. Jutif*, vol. 6, no. 2, pp. 741–754, Apr. 2025, doi: 10.52436/1.jutif.2025.6.2.2606.

[5] C.-L. Lee, T.-H. Hsu, Y.-T. Wu, W.-Y. Guo, W.-C. Chu, and C.-Y. Lien, "Deep Learning for Content-Based Medical Image Retrieval in Picture Archiving and Communication Systems for Brain Tumor Detection: Algorithm Development and Validation," *JMIR Med. Inform.*, vol. 14, pp. e78300–e78300, Apr. 2026, doi: 10.2196/78300.

[6] J. Choe *et al.*, "Content-based Image Retrieval by Using Deep Learning for Interstitial Lung Disease Diagnosis with Chest CT," *Radiology*, vol. 302, no. 1, pp. 187–197, Jan. 2022, doi: 10.1148/radiol.2021204164.

[7] El Houby and E. M. F, "COVID-19 detection from chest X-ray images using transfer learning," *Sci. Rep.*, vol. 14, no. 1, p. 11639, May 2024, doi: 10.1038/s41598-024-61693-0.

[8] M. Abdullah, F. berhe Abrha, B. Kedir, and T. Tamirat Tagesse, "A Hybrid Deep Learning CNN model for COVID-19 detection from chest X-rays," *Heliyon*, vol. 10, no. 5, p. e26938, Mar. 2024, doi: 10.1016/j.heliyon.2024.e26938.

[9] G. Gautam and A. Khanna, "Content Based Image Retrieval System Using CNN based Deep Learning Models," *Procedia Comput. Sci.*, vol. 235, pp. 3131–3141, Jan. 2024, doi: 10.1016/j.procs.2024.04.296.

[10] M. Bundea and G. M. Danciu, "Pneumonia Image Classification Using DenseNet Architecture," *Information*, vol. 15, no. 10, p. 611, Oct. 2024, doi: 10.3390/info15100611.

[11] P. Rajpurkar *et al.*, "CheXNet: Radiologist-Level Pneumonia Detection on Chest X-Rays with Deep Learning," Dec. 25, 2017, *arXiv*: arXiv:1711.05225. doi: 10.48550/arXiv.1711.05225.

[12] A. C. Yadav and M. H. Kolekar, "Deep feature-based approaches for brain tumor classification and segmentation in medical imaging," *Biomed. Signal Process. Control*, vol. 117, p. 109603, May 2026, doi: 10.1016/j.bspc.2026.109603.

[13] M. M. Kabir, M. F. Mridha, A. Rahman, Md. A. Hamid, and M. M. Monowar, "Detection of COVID-19, pneumonia, and tuberculosis from radiographs using AI-driven knowledge distillation," *Heliyon*, vol. 10, no. 5, p. e26801, Mar. 2024, doi: 10.1016/j.heliyon.2024.e26801.

[14] M. Singh and M. K. Singh, "Content based medical image retrieval using deep learning and handcrafted features in dimensionality reduction framework," *Comput. Electr. Eng.*, vol. 127, p. 110581, Oct. 2025, doi: 10.1016/j.compeleceng.2025.110581.

[15] H. M. S. S. Herath, H. M. K. K. M. B. Herath, N. Madusanka, and B.-I. Lee, "A Systematic Review of Medical Image Quality Assessment," *J. Imaging*, vol. 11, no. 4, p. 100, Apr. 2025, doi: 10.3390/jimaging11040100.

[16] M. Ehrgott, M. Köksalan, M. Kadziński, and K. Deb, "Fifty years of multi-objective optimization and decision-making: From mathematical programming to evolutionary computation," *Eur. J. Oper. Res.*, vol. 330, no. 1, pp. 1–25, Apr. 2026, doi: 10.1016/j.ejor.2025.06.012.

[17] R. O'Shea, P. Deeney, E. Triantaphyllou, L. Diaz-Balteiro, and S. Armagan Tarim, "Weight stability intervals for multi-criteria decision analysis using the weighted sum model," *Expert Syst. Appl.*, vol. 296, p. 128460, Jan. 2026, doi: 10.1016/j.eswa.2025.128460.

[18] K. Yonekura, R. Yamada, S. Ogawa, and K. Suzuki, "Hypervolume-Based Multi-Objective Optimization Method Applying Deep Reinforcement Learning to the Optimization of Turbine Blade Shape," *AI*, vol. 5, no. 4, pp. 1731–1742, Dec. 2024, doi: 10.3390/ai5040085.

[19] R. Shetty, V. S. Bhat, and J. Pujari, "Content-based medical image retrieval using deep learning-based features and hybrid meta-heuristic optimization," *Biomed. Signal Process. Control*, vol. 92, p. 106069, Jun. 2024, doi: 10.1016/j.bspc.2024.106069.

[20] N. E. I. Karabadji, A. Amara Korba, A. Assi, H. Seridi, S. Aridhi, and W. Dhifli, "Accuracy and diversity-aware multi-objective approach for random forest construction," *Expert Syst. Appl.*, vol. 225, p. 120138, Sep. 2023, doi: 10.1016/j.eswa.2023.120138.

Vol. 7, No. 3, June 2026, Page. 2439-2450
https://jutif.if.unsoed.ac.id
DOI: https://doi.org/10.52436/1.jutif.2026.7.3.5884

[21] X. Zhang, J. Zhao, F. Zhang, and X. Chen, "A deep learning method for medical image quality assessment based on phase congruency and radiomics features," *Opt. Lasers Eng.*, vol. 186, p. 108772, Mar. 2025, doi: 10.1016/j.optlaseng.2024.108772.

[22] B. Nirupama, B. S. Dhevdharsan, U. Shreya Reddy, J. Joshan Athanesious, and S. Kiruthika, "Diagnosis based image quality assessment and enhancement for low dose CT image," *Front. Radiol.*, vol. 5, Dec. 2025, doi: 10.3389/fradi.2025.1704113.

[23] A. Breger *et al.*, "A Study of Why We Need to Reassess Full Reference Image Quality Assessment with Medical Images," *J. Imaging Inform. Med.*, vol. 38, no. 6, pp. 3444–3469, Dec. 2025, doi: 10.1007/s10278-025-01462-1.

[24] X. Zhang and H. Cavusoglu, "Skyline operators in multi-criteria decision making: A review of characterization, comparison, and perspectives," *Expert Syst. Appl.*, vol. 306, p. 130889, Apr. 2026, doi: 10.1016/j.eswa.2025.130889.

[25] X. Cui, L. Dong, G. Sun, Y. Huang, Y. Chai, and Q. Yu, "A novel multi-objective SKG-skyline algorithm integrating spatial keyword data transformation," *Complex Intell. Syst.*, vol. 12, no. 5, p. 145, Mar. 2026, doi: 10.1007/s40747-026-02282-8.

[26] K. Yonekura, R. Yamada, S. Ogawa, and K. Suzuki, "Hypervolume-Based Multi-Objective Optimization Method Applying Deep Reinforcement Learning to the Optimization of Turbine Blade Shape," *AI*, vol. 5, no. 4, pp. 1731–1742, Dec. 2024, doi: 10.3390/ai5040085.

[27] M. Ehrgott, M. Köksalan, M. Kadziński, and K. Deb, "Fifty years of multi-objective optimization and decision-making: From mathematical programming to evolutionary computation," *Eur. J. Oper. Res.*, vol. 330, no. 1, pp. 1–25, Apr. 2026, doi: 10.1016/j.ejor.2025.06.012.

[28] M. E. H. Chowdhury *et al.*, "Can AI Help in Screening Viral and COVID-19 Pneumonia?," *IEEE Access*, vol. 8, pp. 132665–132676, 2020, doi: 10.1109/ACCESS.2020.3010287.